

Interacting jammed granular systems

Sára Lévay^{*1}, David Fischer², Ralf Stannarius², Ellák Somfai³, Tamás Börzsönyi³, Lothar Brendel⁴, and János Török^{1,5}

¹*Department of Theoretical Physics, Budapest University of Technology and Economics, H-1111 Budapest, Hungary*

²*Institute of Physics, Otto von Guericke University, D-39106 Magdeburg, Germany*

³*Institute for Solid State Physics and Optics, Wigner Research Centre for Physics, H-1525 Budapest, Hungary*

⁴*Faculty of Physics, University of Duisburg-Essen, D-47048 Duisburg, Germany*

⁵*MTA-BME Morphodynamics Research Group, Budapest University of Technology and Economics, H-1111 Budapest, Hungary*

December 22, 2024

Abstract

Sam Edwards more than 30 years ago proposed a model to describe the statistics of granular packings by an ensemble of equiprobable jammed states. Experimental tests of this model remained scarce so far. We introduce a simple system to analyse statistical properties of jammed granular ensembles to test Edwards' theory. Identical spheres packed in a nearly two-dimensional geometrical confinement were studied in experiments and numerical simulations. When tapped, it evolves towards a ground state, but due to incompatible domain structures it gets trapped. Analytical calculations reproduce relatively well our simulation results, which allows us to test Edwards' theory on a coupled system of two subsystems with different properties. We find that the joint system can only be described by a common compactivity if the stress equilibrium is also taken into account. The results show some counterintuitive effects, as the side with less free volume compactifies.

For a statistical description of arrangements of solid macroscopic particles and for an analysis of the probabilities that certain states are realised by the ensemble, Boltzmann statistics are commonly not suitable. Granular packings are athermal, and the systems cannot explore configuration space by thermal fluctuations. In consideration of this, Sir Sam Edwards proposed an ensemble of equiprobable jammed states to describe granular packings¹. The seemingly contradictory concept of describing static jammed states using equilibrium statistical physics had a mixed reception at first, but recent advances showed the strength of it by deriving analytically the phase space of the random packing including the packing fraction of random close and loose packing².

The calculation of the partition function of the Edwards volume^{1,3} and stress ensemble⁴ is difficult, and up to now was done only in a limited number of cases. Two notable exceptions are random packing of spheres and circles^{2,5–10}, and two-dimensional narrow channels^{11,12}. Direct experimental and numerical verification of calculated properties are even more scarce^{6,12}. In this paper, we consider a system where the partition function can be expressed analytically, and calculated expectation values of measurables agree well with the experiments and simulations.

Another important aspect which we focus on is the interaction of jammed systems. The statistical theory of Edwards is in principle an ideal framework for such coupled systems, but up to now there is hardly any result regarding equilibria of jammed systems^{6,13}. We will show that the denomination 'compactivity' of the control parameter can be misleading: In certain cases, a subsystem with higher compactivity will expand rather than the connected one with smaller compactivity. Nevertheless, the interaction of the two subsystems can be described by the Edwards ensemble.

The system studied here consists of identical spheres. They are contained in a flat rectangular cuboid box with dimensions (L, W, H) in the (x, y, z) directions with gravity in the z direction. If the width W is only slightly larger than the particle diameter (d_p), namely $d_p < W < 1.45d_p$, a ground state of the system in the $x-z$ plane is still an, although slightly

distorted, triangular lattice, with alternating stripes of particles touching the front and back walls in the y direction (see Fig. 1 top). Thus the system can be treated in a two-dimensional description.

In the following, we use dimensionless lengths, in units of the particle diameter $d_p=1$. Starting from a random configuration, the system begins to evolve when it is shaken periodically in z direction. The states of the system between the shaking periods are jammed and thus they are ideal candidates for an Edwards ensemble. In earlier publications, it was shown that the shaken system evolves towards the ground state but the dynamics slows down and the configurations apparently get stuck in metastable states^{12,14}. Snapshots of the jammed states between excitation phases are presented in the Supplementary Figs. S1 and S2 and in the Supplementary Movies for both experiments and simulations. Note that a substantial amount of experimental data has been collected in colloidal systems as well^{15–18}.

It was shown in Ref. ¹⁴ that the system can be described by 13 local particle configurations of a central particle and its 6 neighbours as shown in the bottom of Fig. 1. The ground state is compatible with configurations 4 and 5 only (stripes of particles touching alternatively the back and front wall), so the statistical weight of these configurations, $\rho_{4,5}$, can serve as an order parameter of the system. The different configurations have theoretical minimal areas (sphere centres projected into the $x-z$ plane), which were determined using simulated annealing. As area, we consider the area of the Voronoi cell of the central particle of a given configuration. Areas corresponding to the tightest packings are shown in Fig. 1.

The system can be treated as two-dimensional, since the third dimension (y) is only relevant for the selection of local configurations. The global volume is determined by the (x, z) positions of the particles and thus the relevant quantity is the area of the system in the $x-z$ plane. The volume is considered to be $(1 + \delta)d_p$ times the area of a given subsystem.

Results

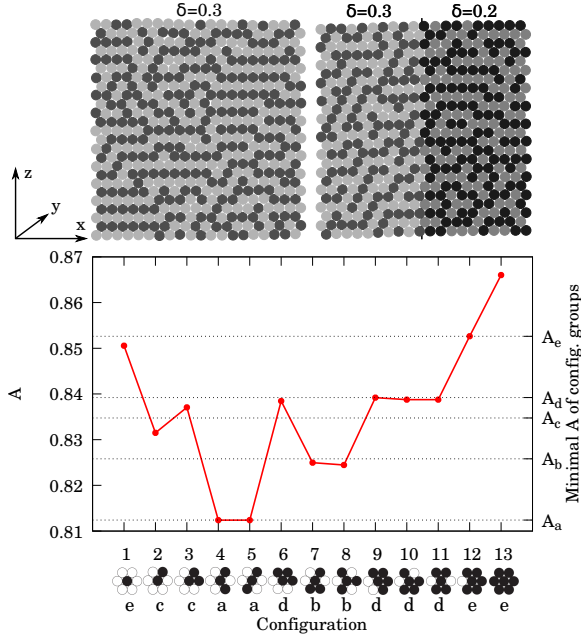


Fig. 1: Sample systems, configuration areas and areas corresponding to the tightest packings. **Top:** sample parts of the system for the normal cell (uniform width) (left) and for the coupled cell with different width (right). **Bottom:** The 13 local configurations (designation see bottom line) of the packed spheres. Dark and bright circles indicate positions at opposite cell plates. All these configuration states are degenerate, they are found twofold with the central particle positioned either at the rear or front cell wall. Most of the configurations are also found in rotated or mirrored forms. The minimal possible Voronoi area of the central particle of the given configuration is shown by the red curve (for $\delta=0.3$), calculated by kinetic Monte Carlo simulation. A_i -s on the right hand side are the minimal Voronoi areas associated with the five configuration groups defined in the text.

Introduction of configuration groups. As shown in Fig. 1, the minimal area of certain subsets of configurations is (almost) the same and we can define configuration groups to facilitate the mean field analysis as follows: $a=\{4, 5\}$, $b=\{7, 8\}$, $c=\{2, 3\}$, $d=\{6, 9, 10, 11\}$, $e=\{1, 12, 13\}$. (Note that configuration 13 is practically non-existent, and $\rho_a=\rho_{4,5}$ is the order parameter.) The corresponding minimal Voronoi area of the central particle in a configuration can be approximated by the following discrete values using the areas $A_1=\sqrt{3}/12$ and $A_2=\sqrt{3-4\delta^2}/12$. These are areas of triangles discussed in detail in¹⁴: A_1 is the third of an equilateral triangle formed by three particles touching the same cell side, while A_2 corresponds to the third of an isosceles triangle with one particle located at the opposite cell side than the others. (So the Voronoi area of a perfect configuration 13 would be $6A_1$.) The minimal area associated with the above configuration groups can be approximated by $A_a=6A_2$, $A_b=4.5A_2+1.5A_1$, $A_c=3.5A_2+2.5A_1$, $A_d=3A_2+3A_1$ and $A_e=1.5A_2+4.5A_1$, shown as dotted lines in Fig. 1.

Elementary processes during shaking. In our study, we use the following assumption: The system is considered to be in a (slightly distorted) triangular lattice in the $x-z$ plane with one principal direction parallel to the x axis. The spheres touch either the front or rear wall in the y direction. During shaking, the following processes are possible: (i) horizontal lines gain or lose one particle, (ii) a particle changes its y position (switches side), (iii) particles move horizontally. The process (i) has the highest impact on the volume of the system and happens simultaneously in all lines generally due to global slip lines (see Supplementary Movies). Process (ii) allows the particles to use the third dimension and optimise the volume beyond the flat triangular lattice. This optimisation is responsible for building up the stripes in the system. This process will create gaps between particles which permits the further compaction of the system by allowing the next layer of particles to occupy some of the released volume. Process (iii) moves the par-

ticles left or right within the line, which has no real influence on the global volume (up to first order in gap size relative to the particle diameter). However, it contributes to the degeneracy of an observed configuration.

Canonical Edwards volume ensemble. The configurational statistics were found, experimentally as well as in the simulations, to be independent of z (and hence of pressure). Thus, we regard a row of N particles as an independent sub-system described by the canonical Edwards volume ensemble and the whole system as a sample from the grand canonical ensemble. Let L be the length of the container in the x direction, M be the total number of particles, and by ρ_i ($i \in \{a, b, c, d, e\}$) we denote the fraction of the different configuration groups in the system. The statistical weight for a given N and configuration fractions ρ_i reads

$$P(N, [\rho_i]) = g_s g_c e^{-(V_{2d} - V_f)/X + J \sum_{i,j} C_{ij} \rho_i \rho_j} \quad (1)$$

with V_f being the volume freed due to increasing packing fraction in the row (thus, $V_f = 0$ denotes the state of maximal wasted volume), while $V_{2d} = (\sqrt{3}/2)d_p LM/N$ is the volume of the perfectly ordered two-dimensional system. The impact of volume change is governed by the compactivity X (corresponding to temperature in equilibrium statistics). Volume also enters via the prefactor g_s , which describes the entropical gain resulting from the possibility of distributing the extra space between the particles. The second prefactor, g_c , takes care of the combinatorial degeneracy of the configurations. The J -term, where i and j run over $\{a, b, c, d, e\}$, finally describes an entropical contribution due to the incompatibility of overlapping configurations. That means, C_{ij} is the number of different ways (disregarding symmetry) in which configurations from the groups i and j can be placed overlapping next to each other. They were determined by enumerating all possible placements of particles in a two-shell hexagon (19 particles).

We calculate all terms analytically. Let $n_i = N \rho_i$ be the number of configurations from group i in a line. An interesting question is the relation between the

configuration distribution ρ_i and the volume. Due to gravity, the configurations from Fig. 1 will be flattened. The extra space in the horizontal direction is thus not wasted but freed to allow for compaction. In linear approximation, this amounts to

$$V_f = \frac{\sqrt{3}}{2} d_p L - \sum_{i \in \{a, \dots, e\}} n_i V_i. \quad (2)$$

Still there remains volume as empty space between neighbouring particles. The factor g_s accounts for the number of possible ways this can be distributed. Let's discretise length in units of $\Delta\ell$ and define $k \equiv V_f/\Delta\ell$, then

$$g_s([n_i], k) = \binom{N+k}{k}. \quad (3)$$

The problem with this term is that it diverges for $\Delta\ell \rightarrow 0$. In Eq. 1, a factor depending only on N is of no importance, because when calculating averages for fixed N , it cancels out. Hence, we renormalise $g_s([n_i], k)$ with $g_s([N, 0, 0, 0, 0], k')$, i.e. the ground state with just configurations from group a in the system and therefore $V_f = V_f(a) = k'/\Delta\ell$, and use

$$\lim_{\Delta\ell \rightarrow 0} \frac{g_s([n_i], k)}{g_s([N, 0, 0, 0, 0], k')} = \left(\frac{k}{k'} \right)^N = \left(\frac{V_f}{V_f(a)} \right)^N \quad (4)$$

as the actual prefactor in P .

The number of different cases for positioning the different configurations in the lattice is:

$$g_c([n_i]) = \frac{N!}{n_1! n_2! n_3! n_4! n_5!}. \quad (5)$$

The task is now straightforward: We have to calculate P for all possible values of N and all possible combinations of $\{n_i\}$ for given N . At first it seems from Eq. (1) that we have two parameters to fit, J and X . However, J should be a globally fixed parameter with which all test results are best fitted with the single remaining parameter, the compactivity X . With C_{ij} defined as above, the best fits were found with $J = 5 \cdot 10^{-7}$. In the following, we will evaluate the results of the Edwards model and compare it to simulations and experiments which we describe briefly here.

Experiments and discrete element method simulations. We used the LIGGGHTS¹⁹ discrete element method (DEM) simulations to study the system. A detailed description can be found in Ref.¹⁴ and in the Methods section. In the cuboid cell, we simulated ~ 6000 particles with periodic boundary conditions in the x direction. The width W of the cell was varied in the range $1.15 d_p \dots 1.4 d_p$. The length of the cell was exactly 69 times the diameter d_p of the particles. As initial conditions, we arranged the particles into a triangular lattice with (i) random y positions and (ii) ordered y positions: a striped pattern of particles touching either the front or the rear wall. The gravitation was varied between $1 g$ and $10 g$. In order to simulate the shaking process, particles were lifted up and released to fall down. This resulted in different agitation energies in the range $3 mgd_p \dots 100 mgd_p$ (m is the particle mass). In Supplementary Movie 2, snapshots of a simulation can be seen.

Ref.¹⁴ and the Methods section provide a detailed description of the experimental setup. Images of the jammed states between shaking periods can be seen in Supplementary Movie 1.

Calculations according to the canonical ensemble The first quantity we calculate is the number of particles per row:

$$\langle N \rangle = \frac{\sum_{N=0}^{\infty} \sum_{\{[n_i]\}} N P(N)}{\sum_{N=0}^{\infty} \sum_{\{[n_i]\}} P(N)}. \quad (6)$$

Surprisingly, we get $\langle N \rangle \simeq L$ with high accuracy especially for low compactivity. It means that on average we should observe a quasi two-dimensional system, which has exactly as many particles as the strictly two-dimensional system would have. In all our experiments and simulations, we observed this law. We have performed simulations by compressing or expanding the simulated container in the x direction and let the particles reorganise to accommodate to the new container size, and we recovered this result. This was also the case when we started from a perfect lattice with striped initial y positions with some extra space in the x direction. The same result was observed independently of the agitation strength (varied

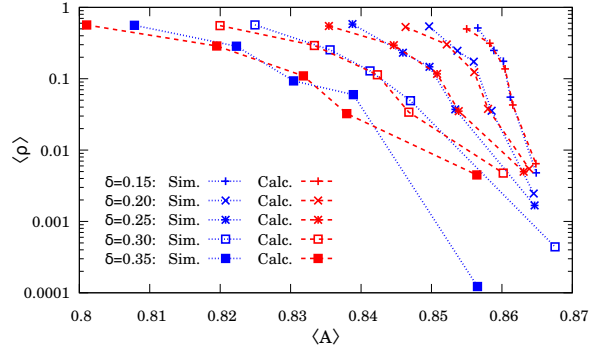


Fig. 2: The dependence of calculations and DEM simulations on the excess cell thickness δ . Configuration group density versus average area for the five configuration groups for different cell thicknesses. **Blue (dotted):** simulation, **red (dashed):** calculation. Fitted values of compactivity: $X(\delta=0.15) = 0.0231$, $X(\delta=0.20) = 0.0228$, $X(\delta=0.25) = 0.0224$, $X(\delta=0.30) = 0.0229$, $X(\delta=0.35) = 0.0232$.

in the experiments) and gravity (varied in the simulations). So from now on in all calculations we fix $N=L$ and all results presented will be done in the canonical ensemble.

Calculations reproducing observations and the dependence on δ . In experiments and simulations, we can determine two average quantities: $\langle A_i \rangle$ and $\langle \rho_i \rangle$, where the former is the average Voronoi area of configuration group i including the extra space around the central particle. The latter is simply the frequency of occurrences of the group. In Fig. 2, we plot $\langle \rho_i \rangle$ versus $\langle A_i \rangle$ from simulations with different values of δ and from calculations which were performed with X best fitting the order parameter ρ_a . One can see that the calculated values reproduce well the observations and the dependence on δ .

The fitted values of X in the simulations (Fig. 2) coincide within a 1.7 % uncertainty ($X=0.0228 \pm 0.004$). It seems that after 100 shakes, systems of different width can be described by the same compactivity even though the order parameter is different (wider systems are more ordered). Note, that such point was not found in experiments.

Incompatible domain structure can be described by Monte Carlo simulations. An intriguing question is: what sets the compactivity in our system? As the system is agitated, X is decreasing but its decrease slows down enormously around the above values. Looking at snapshots of our system (see Supplementary Information), one can see that the evolution of the system formed domains of perfectly ordered subsystems, but these subsystems are either incompatible with each other (different stripe structures) or divided by seemingly stable boundary structures.

It seems that the system develops a metastable domain structure which prevents it from reaching the ground state. In order to verify this, we use the Monte Carlo model introduced in¹⁴. In this dynamics, we consider a system of two state spins (spheres) in a triangular lattice, where the energy is defined by the sum of the minimal Voronoi area of the resulting configurations. The elementary step of the dynamics is a particle switch from one side of the cell to the other. Here, we ran the simulation, instead of in a temperature controlled way, by allowing volume changes up to a maximal limiting value. In Fig. 3, we show the order parameter of the system as function of the maximum allowed volume change dA , normalised by the difference $A_1 - A_2 > 0$ (which is just the difference between the area of the equilateral and isosceles triangles for a given δ). $dA < 0$ means we allow changes only if the total area is reduced by an amount greater than $|dA|$, while $dA > 0$ means we allow slightly unfavourable changes as well: only changes which are increasing the total area by an amount greater than dA are suppressed. One can observe a monotonically increasing stepped curve shown in Fig. 3. The ground state, which corresponds to $X=0$, is not reached at $dA=0$. In order to compactify our frustrated system further one needs to allow unfavourable moves ($\Delta A > 0$). This is responsible for the slow dynamics of the system. Furthermore it also hinders the calculation of the compactivity of a particular system: in narrow systems the volume difference between the configurations is too small to drive the system efficiently towards the ground state. Details of the Monte Carlo model can be found in the Methods section.

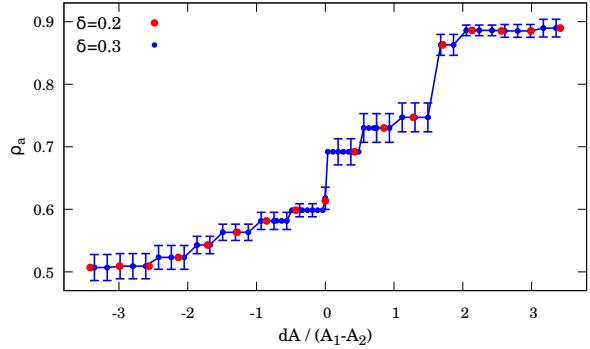


Fig. 3: Monte Carlo model describing the slow dynamics. The order parameter (the statistical weight of configurations 4 and 5 (configuration group a) as function of the maximal allowed area change (normalised by $A_1 - A_2$) in the Monte Carlo model for $\delta=0.2$ (red) and $\delta=0.3$ (blue). (Each data point is an ensemble average of 10 simulations using a given dA . For the blue data set the standard deviation of different simulations is shown as well, while the red data set is shown only as a validation for different system width, thus the less number of data points.)

Coupling of two jammed subsystems. Our setup allows to perform a unique experiment in which we can bring two well-defined jammed subsystems in contact. This can be done by changing the width (W) of the cell in one half of the system. This has been done both in experiments and in simulations (see Supplementary Movies) with $\delta=0.2$ and $\delta=0.3$ for the different sides of the cell (in simulations we used periodic boundary conditions in the x direction). For simulations, we used the same number of shakes as in Fig. 2, so in the homogeneous cell the compactivity is the same for both subsystems, while in the experiments the compactivities of the uncoupled systems were $X(\delta=0.2)=0.0175$ and $X(\delta=0.3)=0.0139$, respectively.

According to the theory, one should be able to describe the system with a common compactivity. From classical correspondence, if one naively assumes equilibration of the compactivities, one would expect higher order and thus a potentially more compact system on the thinner side of the connected system, where the compactivity should decrease, and the op-

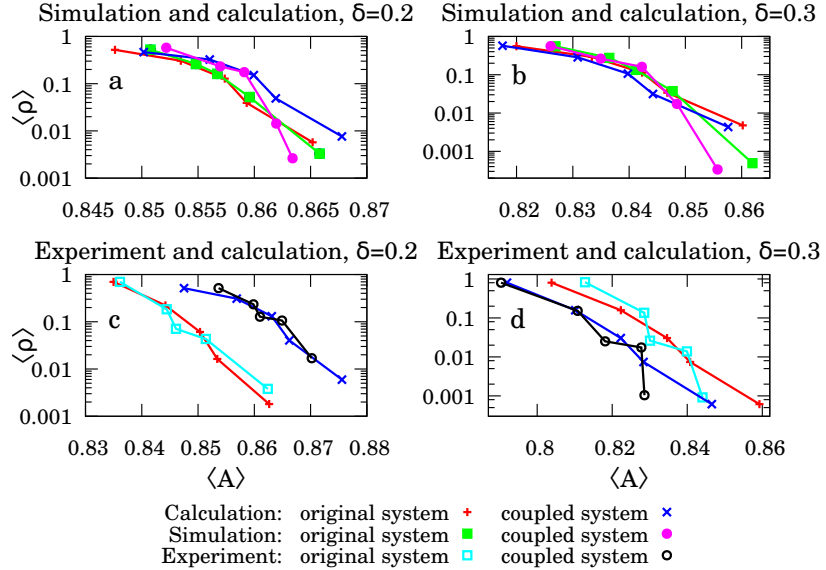


Fig. 4: Effect of coupling on the subsystems compared to the original system. Comparison of the configuration group density versus average area in the original and coupled system for the five configuration groups. **a,b:** comparison of simulation and calculation, **c,d:** comparison of experiment and calculation, **a,c:** for $\delta=0.2$, **b,d:** for $\delta=0.3$.

posite effect in the wider cell partition. In Fig. 4 (c,d), we actually observe the opposite effect.

We can, however calculate the partition function for the complete coupled system with $\delta=0.2$ and $\delta=0.3$ for the two halves. The results are shown in Fig. 4. The curves show more fluctuation, since the half system has a larger relative error, but the trends seem to be the same as in the simulated data. Note also that there was a slight difference in the excess cell thicknesses δ between pure and coupled systems in experiments which was taken into account in the calculation.

Coupling and mechanical stability. We find that the coupled system can be very well described by the volume ensemble alone, but it cannot be put together by taking the two subsystems at the common compactivity. The reason is that in the coupled case the system would not be in mechanical equilibrium in the jammed state. The configurations of the narrower system take more area and have higher pres-

sure at the sides than those of the wider system. This is the reason behind the volume change of the two sides, the dilution of the narrow system and the compaction of the wider.

In Ref.² the authors clearly point out that the volume ensemble is only valid if the system is in a mechanically stable jammed configuration. Thus the coupled system will change to fulfil the force equilibrium constraint. If the system violates this, then the results from subsystems cannot be applied to the whole system.

In our case, it is easy to take into account the stress equilibrium: The rows must be at the same height in both side of the system. This means the narrower part must contract and the other half must expand. Thus we can use our canonical ensemble calculation, but instead of $L/2$ as system width on both sides we use the widths determined from the coupled calculation which means a 3% shift in benefit of the narrower part. If we redo the calculations in the canonical ensemble for the partial systems with the above calculated system lengths and using the com-

mon compactivity, then we get results which are basically indistinguishable from the ones obtained from the coupled system. This suggests that the volume ensemble for the coupled system can only be applied if the coupling does not change the mechanical stability of the jammed state, or if it can be taken into account easily.

Discussion

In summary, we have shown that a simple system consisting of uniform beads in a nearly two-dimensional cell is an excellent example to be described by the Edwards ensemble. The observables can be calculated exactly and the calculation matches reasonably well with experiments. We have shown that the system cannot reach its ground state due to frustration in the domain structure which can only be dissolved through unfavourable events with very small probability. Our results raise a new question: what sets the apparent compactivity of the system?

We have also tested the applicability of the Edwards ensemble for two coupled subsystems. We found that the resulting system can only be described if the stress ensemble is also taken into account, in which case the observables were recovered with good accuracy using a common compactivity.

Methods

Discrete Element Method simulations. The simulations were implemented using the LIGGGHTS¹⁹ DEM method, consisting of a cell with sizes $(69d_p, W, \sim 75d_p)$, where the width W of the cell was varied between $1.15d_p$ and $1.4d_p$. Periodic boundary conditions were applied in the x direction. Walls had the same mechanical and frictional properties as the grains. The cell was filled with ~ 6000 spherical particles with uniform diameter d_p . As initial filling we applied two different methods: We arranged the particles into a triangular lattice with (i) random y positions and (ii) ordered y positions: a striped pattern of particles touching either the front or rear wall. (In Ref.¹⁴ it is

compared with simulations using completely random initial filling.)

In order to simulate shaking, particles were lifted up and released to fall down. The strength of gravitation was varied between $1\ g$ and $10\ g$, so the agitation energy was in the range $3\ mgd_p$ and $100\ mgd_p$. The equilibrated configuration of particles after each shaking period is considered as a jammed state, a sample from the Edwards ensemble. The grains are interacting when in contact via the Hertz model. The mechanical and frictional properties of particles were also varied: the coefficient of restitution between $0.25 \dots 0.75$, the coefficient of friction between $0.0 \dots 0.2$, and the Young modulus between $5 \cdot 10^6\ \text{Pa} \dots 5 \cdot 10^8\ \text{Pa}$. Changing these parameters had no considerable effect on the results studied in this paper. A more detailed description can be found in¹⁴.

Experiments. In experiments we used vertical sandwich cells. The walls were made from glass plates and 3D printed borders. The size of the cell was $(140\ \text{mm}, W, 140\ \text{mm})$, the width W was varied between $1.2d_p$ and $1.3d_p$. For the coupled case two transparent sheets were glued to one half of the glass plates to reduce the width of the cell. Precision glass spheres with a diameter $d_p = 2.0 \pm 0.02\ \text{mm}$ were placed randomly in the cell by gravitational filling from the top. A sinusoidal signal generated by the voice coil was applied as agitation, vertical vibration of the cell. Amplitude and frequency of the signal were varied leading to vertical accelerations between $1\ g$ and $5\ g$, measured by an acceleration sensor. After each shaking period, a photo from the current jammed state was taken. Uniform background illumination allowed the clear distinction of particles located at the front and rear side of the cell by their brightness. The positions of particles and resulting configurations were determined by image analysis. A series of images of the jammed states in the coupled cell can be seen in Supplementary Movie 1.

Monte Carlo model. Monte Carlo simulations were performed to test the effect of mechanism (ii) in the compactification (particle switches side). We were interested in the question whether the system

can reach its striped ground state by particles switching sides.

To this end we made a model where the particles were placed in a triangular lattice. The volume of the system was determined by the sum configuration volume of all particles as given by the minimal volume in Fig. 1.

We have created a Metropolis algorithm using particles switching sides as elementary step and the complete volume of the system as energy. It turned out that the system compactifies more at finite temperature than at zero. To measure the volume of the necessary unfavourable elementary steps for further compaction we have run the system instead of temperature at energy control, namely we have accepted elementary steps with volume change less than ΔV . The results of the simulations are shown in Fig. 3.

Data availability

The datasets generated and/or analysed during the current study are available from the corresponding author on reasonable request.

References

1. Sam F Edwards and RBS Oakeshott. Theory of powders. *Physica A*, 157(3):1080–1090, 1989.
2. Adrian Baule, Flaviano Morone, Hans J Herrmann, and Hernán A Makse. Edwards statistical mechanics for jammed granular matter. *Rev. Mod. Phys.*, 90(1):015006, 2018.
3. Anita Mehta and SF Edwards. Statistical mechanics of powder mixtures. *Physica A*, 157(3):1091–1100, 1989.
4. Raphael Blumenfeld and Sam F Edwards. Geometric partition functions of cellular systems: Explicit calculation of the entropy in two and three dimensions. *Eur. Phys. J. E*, 19(1):23–30, 2006.
5. Volker Becker and Klaus Kassner. Protocol-independent granular temperature supported by numerical simulations. *Phys. Rev. E*, 92(5):052201, 2015.
6. James G Puckett and Karen E Daniels. Equilibrating temperaturelike variables in jammed granular subsystems. *Phys. Rev. Lett.*, 110(5):058001, 2013.
7. Song-Chuan Zhao and Matthias Schröter. Measuring the configurational temperature of a binary disc packing. *Soft Matter*, 10(23):4208–4216, 2014.
8. Vasili Baranau, Song-Chuan Zhao, Mario Scheel, Ulrich Tallarek, and Matthias Schröter. Upper bound on the edwards entropy in frictional monodisperse hard-sphere packings. *Soft Matter*, 12(17):3991–4006, 2016.
9. Alain Barrat, Jorge Kurchan, Vittorio Loreto, and Mauro Sellitto. Edwards’ measures for powders and glasses. *Physical Review Letters*, 85(24):5034, 2000.
10. Rémi Monasson and Olivier Pouliquen. Entropy of particle packings: an illustration on a toy model. *arXiv preprint cond-mat/9702027*, 1997.
11. Richard K Bowles and S S Ashwin. Edwards entropy and compactivity in a model of granular matter. *Phys. Rev. E*, 83(3):031302, 2011.
12. Ramiro M Irastorza, C Manuel Carlevaro, and Luis A Pugnaloni. Exact predictions from the edwards ensemble versus realistic simulations of tapped narrow two-dimensional granular columns. *J. Stat. Mech.: Theor. Exp.*, 2013(12):P12012, 2013.
13. Matthias Schröter, Daniel I Goldman, and Harry L Swinney. Stationary state volume fluctuations in a granular medium. *Phys. Rev. E*, 71(3):030301(R), 2005.
14. Sára Lévy, David Fischer, Ralf Stannarius, Balázs Szabó, Tamás Börzsönyi, and János Török. Frustrated packing in a granular system under geometrical confinement. *Soft Matter*, 14(3):396–404, 2018.
15. Yilong Han, Yair Shokef, Ahmed M Alsayed, Peter Yunker, Tom C Lubensky, and Arjun G Yodh. Geometric frustration in buckled colloidal monolayers. *Nature*, 456(7224):898–903, 2008.
16. Yair Shokef and Tom C Lubensky. Stripes, zigzags, and slow dynamics in buckled hard spheres. *Phys. Rev. Lett.*, 102(4):048303, 2009.

17. Yair Shokef, Anton Souslov, and Tom C Lubensky. Order by disorder in the antiferromagnetic ising model on an elastic triangular lattice. *Proceedings of the National Academy of Sciences*, 108(29):11804–11809, 2011.
18. Fabio Leoni and Yair Shokef. Attraction controls the entropy of fluctuations in isosceles triangular networks. *Entropy*, 20(2):122, 2018.
19. Christoph Kloss, Christoph Goniva, Alice Hager, Stefan Amberger, and Stefan Pirker. Models, algorithms and validation for opensource dem and cfd-dem. *Prog. Comp. Fluid Dynamics*, 12(2-3):140–152, 2012.

Additional information

Supplementary information is available for this paper.

Acknowledgments

The authors thank Torsten Trittel for support in the construction of the experimental setup. The study was funded by the Deutsche Forschungsgemeinschaft, DFG, within grant STA 425/38-1, by the Hungarian National Research, Development and Innovation Office (NKFIH), under Grant No. OTKA K 116036, by the BME IE-VIZ TKP2020 program, by DAAD and TEMPUS within the researcher exchange program (Grant No. 274464), and by the ÚNKP-19-3 New National Excellence Program of the Ministry for Innovation and Technology of Hungary.

Author contributions

The concept of the research originated from R.S. The experimental work and the associated data analysis were done by D.F. and supported by S.L. during an exchange visit. DEM simulations and data analysis were done by S.L. Monte Carlo simulations were performed by J.T. and S.L. Theoretical idea and work were achieved by R.S., J.T. and L.B. All authors contributed to the writing of the manuscript.

Competing interests

The authors declare no competing interests.